

Supporting Information

Self-Propelled Chemotactic Ionic Liquid Droplets

Wayne Francis, Cormac Fay, Larisa Florea and Dermot Diamond*

The Insight Centre for Data Analytics, National Centre for Sensor Research,
School of Chemical Sciences, Dublin City University, Dublin, Ireland

*Corresponding author: Larisa.florea@dcu.ie

Table of Contents

- 1. Materials and methods**
- 2. Micro-channel fabrication**
- 3. Surface tension measurements**
- 4. Propulsion mechanism**
- 5. Droplet tracking and gradient analysis**
- 6. Examples of droplet chemotaxis**
- 7. References**

1. Materials and Methods

Hydrochloric acid (HCl) (Sigma-Aldrich® Ireland Ltd), sodium hydroxide (NaOH) (Sigma-Aldrich® Ireland Ltd), Sodium Chloride (NaCl) (Sigma-Aldrich® Ireland Ltd), Dichloromethane (DCM) (Sigma-Aldrich® Ireland Ltd) and 1-(methylamino)anthraquinone red dye (Sigma-Aldrich® Ireland Ltd) were all used as purchased.

The polyacrylamide hydrogel was synthesized by mixing 2.8 mmol of acrylamide (Sigma-Aldrich® Ireland Ltd) with 3 % N,N-Methylenebisacrylamide (mBIS) (Sigma-Aldrich® Ireland Ltd) and 1 % phenylbis(2,4,6-trimethylbenzoyl)phosphine oxide (PBPO) (Sigma-Aldrich® Ireland Ltd), using 500 µl of 4:1 (V:V) dimethyl sulfoxide (DMSO) (Sigma-Aldrich® Ireland Ltd) : deionised water as the solvent. The hydrogel was polymerized for 2 minutes under white light.

The Ionic liquid (IL) trihexyl(tetradecyl)phosphonium chloride ([P_{6,6,6,14}][Cl]) (Sigma-Aldrich® Ireland Ltd) was decolorized by dissolving in 10 ml of dichloromethane. The solution was then treated with activated charcoal and left to reflux at 40°C for 12 hours. The carbon was removed by vacuum filtration, after which it was passed through aluminum oxide (activated, basic, Brockmann, Sigma-Aldrich® Ireland Ltd). Finally the solvent was removed under vacuum for 48 hrs.

Nuclear magnetic resonance (NMR) was performed to determine if the IL was undergoing any chemical reaction with NaOH. ¹H-NMR and ³¹P-NMR spectroscopy was performed using a Bruker Avance® spectrometer (400 MHz). Approximately 10 mg of sample per 1 ml of deuterated chloroform (CDCl₃) (Sigma-Aldrich® Ireland Ltd) was used in the experiments.

2. Micro-channel fabrication

Fabrication of the channels used in this study was carried out using the program AutoCAD 2014 to design the microfluidic platform. A CO₂ laser ablation system (Optec Laser Micro-machining Systems, Belgium) was then used to cut the structures from a 1.1 mm poly(methyl methacrylate) (PMMA) sheet which had a 50 µm double sided pressure sensitive adhesive (PSA) (AR8890, Adhesives Research, Ireland) layer attached. Once cut, the protective layer from the PSA was removed and then the PMMA/PSA layer was laminated with another 1.1 mm PMMA sheet. The final channels were 2 mm wide and 1.1 mm high.

3. Surface tension measurements

Surface tension measurements were performed with a FTA200 Dynamic Contact Angle Analyzer using the pendant drop method.

Various compositions of the solutions used in the study were tested. To test the surface tension effect that the IL surfactant had on each solution, the surface tension of each solution was tested with (c= 1mg/ml) and without the surfactants, see Table S1.

To prepare the solutions for the surface tension measurements, 1 mg of the IL was added to 1 ml of the aqueous solution. This proportion was chosen as it is similar to the quantity of the IL (droplet) per aqueous solution in the fluidic channel.

Table S1. Surface tension measurements of solutions used in the study, with and without the IL surfactant added.

Solution	γ_1 (mN/m)	γ_2 (mN/m)	γ_3 (mN/m)	AVG γ (mN/m)
HCl 10 ⁻² M	74.13	74.39	73.82	74.11
HCl 10 ⁻² M/[P _{6,6,6,14}][Cl]	72.1	72.08	73.51	72.56
HCl 10 ⁻² M/[P _{6,6,6,14}][DCA]	72.92	72.95	73.6	73.16
NaOH 10 ⁻² M	72.39	73.32	73.66	73.12
NaOH 10 ⁻² M/[P _{6,6,6,14}][Cl]	33.29	33.5	33.4	33.40
NaOH 10 ⁻² M/[P _{6,6,6,14}][DCA]	73.48	73.2	72.84	73.17
NaCl 10 ⁻² M	72.45	74.59	74.68	73.91
NaCl 10 ⁻² M/[P _{6,6,6,14}][Cl]	72.62	73.44	73.51	73.19
NaCl 10 ⁻⁵ M	73.96	74.08	74.67	74.24
NaCl 10 ⁻⁵ M/[P _{6,6,6,14}][Cl]	38.24	38.52	38.52	38.43
KBr 10 ⁻² M	71.75	72.67	73.6	72.67
KBr 10 ⁻² M/[P _{6,6,6,14}][Cl]	40.92	39.74	40.75	40.47
KBr 10 ⁻⁵ M	71.85	72.85	72.53	72.41
KBr 10 ⁻⁵ M/[P _{6,6,6,14}][Cl]	34.64	35.12	34.37	34.71
KCl 10 ⁻² M	72.37	71.02	72.86	72.08
KCl 10 ⁻² M/[P _{6,6,6,14}][Cl]	66.31	64.32	66.04	65.56
KCl 10 ⁻⁵ M	69.05	71.88	71.96	70.96
KCl 10 ⁻⁵ M/[P _{6,6,6,14}][Cl]	34.88	34.64	34.68	34.73
NaI 10 ⁻² M	73.94	74.77	73.72	74.14
NaI 10 ⁻² M/[P _{6,6,6,14}][Cl]	59.28	61.58	62.35	61.07
NaI 10 ⁻⁵ M	73.05	73.57	72.81	73.14
NaI 10 ⁻⁵ M/[P _{6,6,6,14}][Cl]	34.46	34.48	34.58	34.51

4. Propulsion mechanism

Although it was previously confirmed that tetraalkylphosphonium halides can be combined with concentrated sodium hydroxide and ammonia without any degradation^{1, 2}, several reports state that tetraalkylphosphonium IL salts are not always stable in the presence of hydroxides or other bases, and may undergo Hoffmann- or β -elimination in the presence of a strong base, which results in the formation of a tertiary phosphine oxide and alkane¹. In order to confirm that the propulsion mechanism of the droplets is due to the triggered release of the surfactant and not due to chemical reaction, the stability of trihexyl(tetradecyl)phosphonium chloride ionic liquid was investigated by analysis of the degradation products formed after mixing the ionic liquid phase with aqueous NaOH. For this, a small amount of the IL (\approx 10 mg) was added to an excess of NaOH 10⁻² M (\approx 1 ml). The solution was stirred overnight and

the product was then extracted with DCM. The DCM was removed by evaporation and a ^{31}P -NMR spectrum of the extraction was recorded.

No increase in the amount of phosphine oxide (resonance signal of phosphine oxide is situated at 49.6 ppm^2) was found on treatment with NaOH, and only the resonance signal of the trihexyl(tetradecyl)phosphonium cation at 32.7 ppm was observed. This indicates that there was no chemical reaction between the NaOH and the droplet.

$[\text{P}_{6,6,6,14}][\text{Cl}]$ ^{31}P NMR (400 MHz, CDCl_3): 32.7 (s, 1P) . (Figure S1)

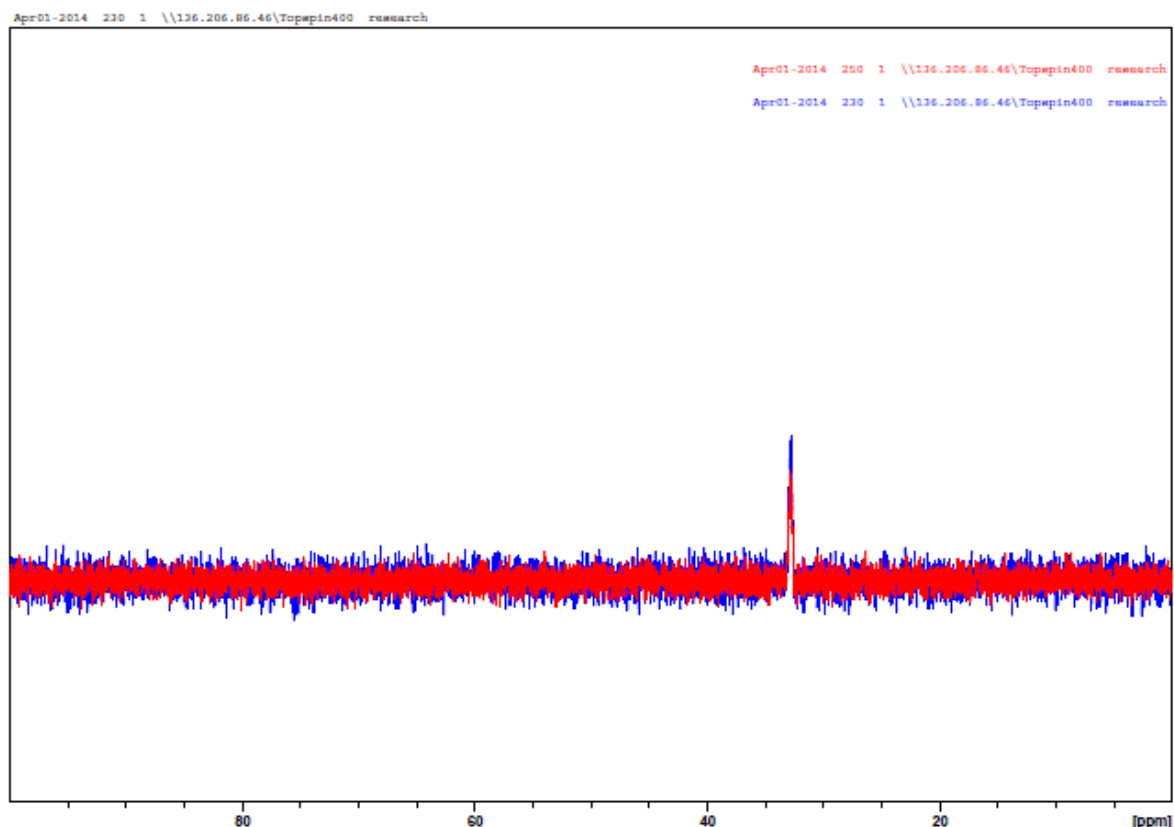


Figure S1. ^{31}P spectra of the cleaned $[\text{P}_{6,6,6,14}][\text{Cl}]$ before (blue) and after extraction (red).

The ^1H NMR spectrum also showed that only the IL was present after the extraction.

$[\text{P}_{6,6,6,14}][\text{Cl}]$ ^1H NMR (400 MHz, CDCl_3): $0.86 - 0.88\text{ (m, 12H, CH}_3)$, $1.2 - 1.3\text{ (d, 32H, CH}_2)$, $1.49\text{ (s, 16H, CH}_2)$, $2.4\text{ (m, 8H, CH}_2)$. (Figure S2)

This is also an indication that no other compound is formed during the propulsion process.

Therefore the chemotactic movement of these droplets is due to surface tension effects which stems from the triggered release of the $[\text{P}_{6,6,6,14}]^+$, a very efficient cationic surfactant which is a constituent of the IL droplet. When the droplet is placed into a Cl^- gradient, there is a biased release of the surfactant from the droplet into aqueous solution. As the surfactant diffuses from the droplet, it causes an asymmetric surface tension gradient around the droplet. This creates a flow of liquid, due to the Marangoni effect, a phenomenon which states that liquid flows from areas of low surface tension to areas of high surface tension. The droplet is thus

driven forward towards the highest concentration of Cl^- in the solution (the source of the chemoattractant). The rate of release of the $[\text{P}_{6,6,6,14}]^+$ surfactant is controlled by the solubility of anion of the IL in the solution.

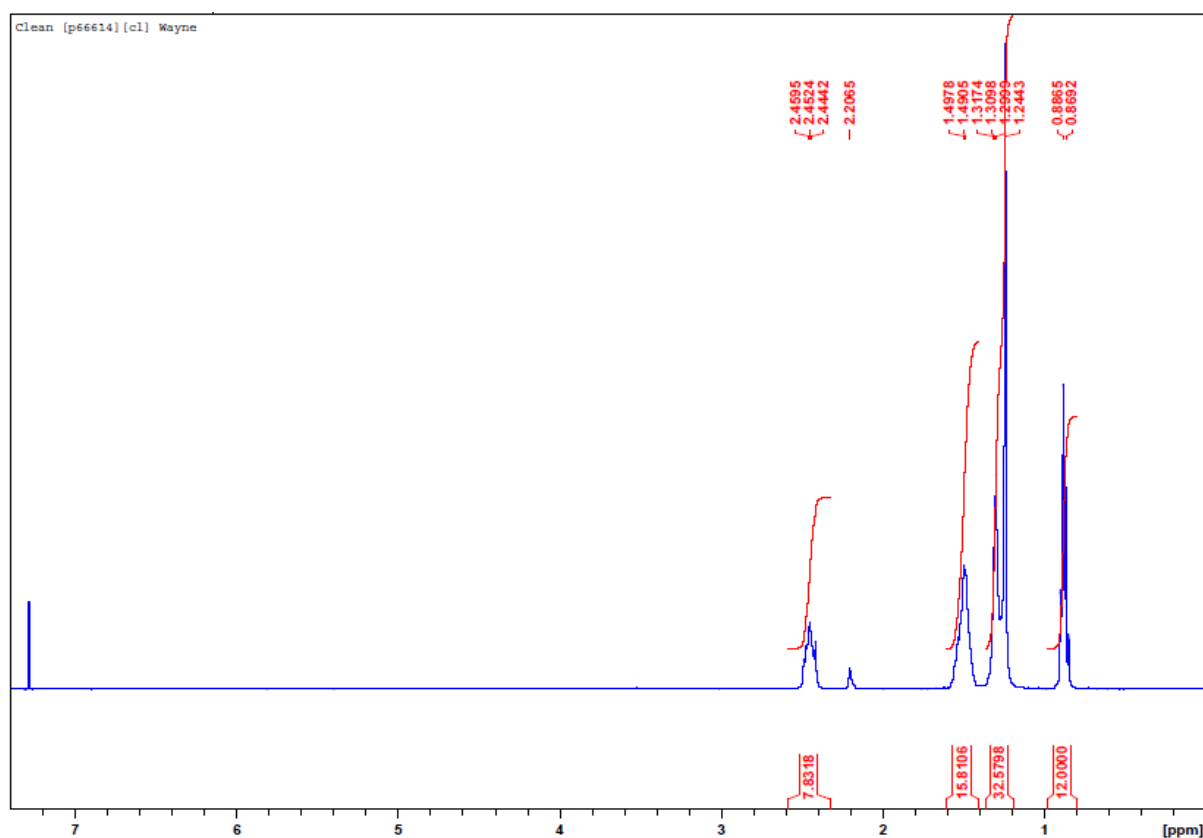


Figure S2. $^1\text{H-NMR}$ spectra of a sample of cleaned $[\text{P}_{6,6,6,14}][\text{Cl}]$, after extraction study.

5. Droplet tracking and gradient analysis

Video S1 presents a captured recording demonstrating a single droplet travelling towards the source of a chemoattractant. At times 4s, 5s and 6s, three droplets of chemoattractant (110 – 170 μl in total) were added to the upper right microfluidic channel (see Figure S5, position a). The chemoattractant was then given 10 s to sufficiently propagate along the channels whereupon at time 16s a single droplet was introduced along the lower right channel (see Figure S5, position b). It can be observed that the droplet begins to travel towards the source of chemoattractant, slowly at first, followed by an increase in speed, until it comes to an eventual stop at the chemoattractant location source. The rate of release of the surfactant from the droplet is dependent on the Cl^- concentration at the IL/aqueous boundary, and the steepness of the Cl^- gradient determines the speed of the droplet.

These observations were investigated by tracking the droplet by means of a custom-written vision system program. This was achieved by firstly controlling the visual environment by separating the background (channels: white/grey – weak in colour intensity) to that of the droplets of interest (droplet: red – strong in colour intensity), see Figure S3 - left. Classification of pixel groups corresponding to the droplet was therefore possible.

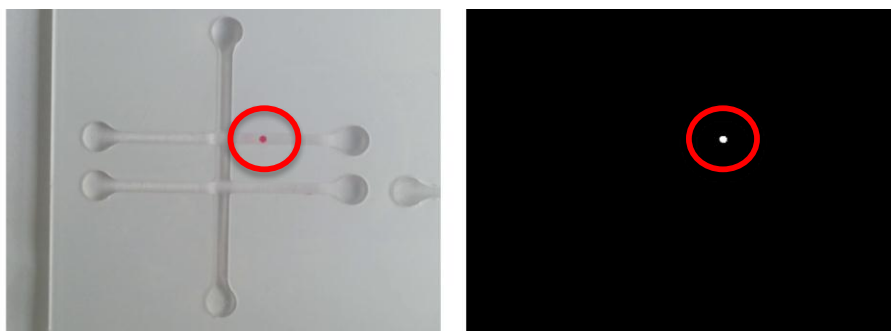


Figure S3. Example of a captured image from Video S1 (left) with processed mask image (right). The droplet position is ringed in both images.

Transformation from the captured sRGB colour space to the HSV colour space allowed for a separation of colour (Hue), colour intensity (Saturation), and light intensity (Value) into their constituent components (3 channels).³ A threshold applied to the S channel resulted in a mask image as shown in Figure S3 (right). Areas of white-connected pixels were grouped together using a connected component analysis algorithm. Information describing each connected region was extracted (e.g. size, shape), which allowed the program to discount noise and/or other artifacts through a series of filters. This formed the basis of a similarity-matching algorithm, which when applied to matching regions in each successive frame allowed tracking of the droplet throughout the video. Data such as the frame in which the droplet appeared and its location (region's centre x, y coordinates) were recorded for later analysis.

During video capturing, the camera was fixed orthogonal to the chip. A conversion of units (from pixels to mm) was therefore possible through the known distance of a straight channel's distal end-points (60 mm) and measurement of corresponding points in captured frames. The distance with which each droplet travelled from frame-to-frame was calculated (using the standard Euclidian algorithm) and the total distance travelled of each droplet was subsequently determined. Finally, using the frame number the time was calculated using the constant captured frame rate of 25 fps set on the capturing device.

The droplet's progress over time from its introduction to the channel, to arrival at the source is presented in Figure S4. The full dataset appears as the grey line within the video, this was down-sampled (every 35th data point) for easier visual reference of the data.

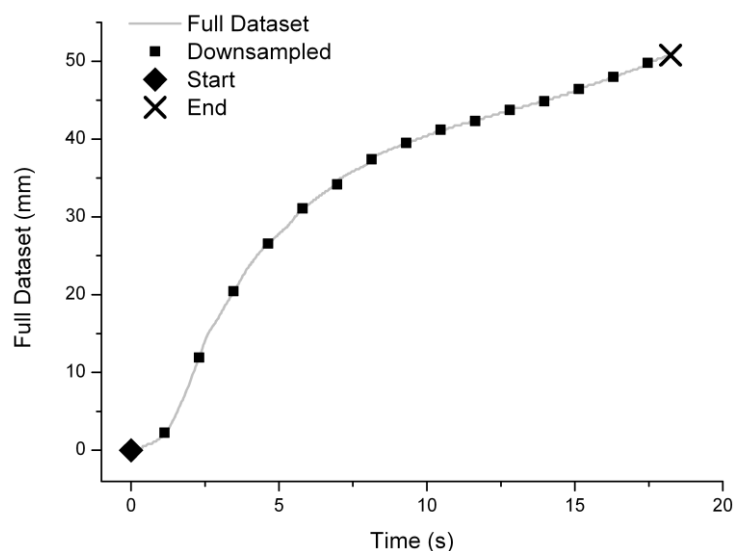


Figure S4. Tracking of the droplet's distance from its point of entry (\blacklozenge, t_0) towards its end position/source of chemoattractant (X), see Video S1. Grey line – full dataset at every video frame. Black squares – down sampled data points from full dataset (every 35th point).

The above approach was expanded to investigate the movement of multiple droplets at different locations within the channel network, see Video S4. In a similar manner to Video S1, a Cl^- ion was created by adding several droplets of $\text{HCl } 10^{-2} \text{ M}$ chemoattractant (point X, Figure S5) to the fluidic network initially filled with a NaOH solution 10^{-2} M , followed by addition of 6 individual droplets at different locations and times, see Figure S5 and Table S2 for details.

The distance travelled by each droplet from their respective entry points to the Cl^- ion source was tracked as a function of time, see Figure S6. In each case the plots resulted in a similar trend as before (Figure S4). The droplets tend to start slow but soon speed up, then slow down again upon arrival at the Cl^- source. For droplets that have a relatively smooth passage from point of entry to the chemoattractant source, the distance travelled as a function of time fits approximately to a sigmoid model. The typical average speed of the droplets over the first 30s is between 0.5-4 mm/s. Variations from this profile *e.g.* droplets b, e, f (Figure S6) may be due to the droplet changing direction at branches in the fluidic network.

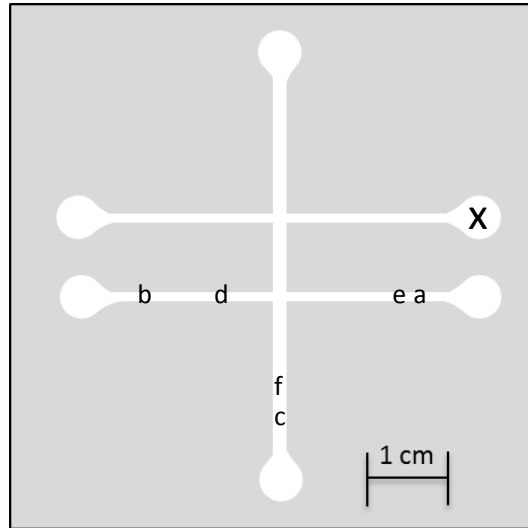


Figure S5. Fluidic network diagram showing the locations where each solution was introduced. (X) Chemoattractant, (a) Droplet a, (b) Droplet b, (c) Droplet c, (d) Droplet d, (e) Droplet e, (f) Droplet f.

Table S2. Description of where and when addition occurred in Video S4, see Figure S5 for location correlation.

Time(s)	Solution Introduced	Location
0	HCl	X
21	Droplet a	a
24	Droplet b	b
27	Droplet c	c
53	Droplet d	d
57	Droplet e	e
61	Droplet f	f

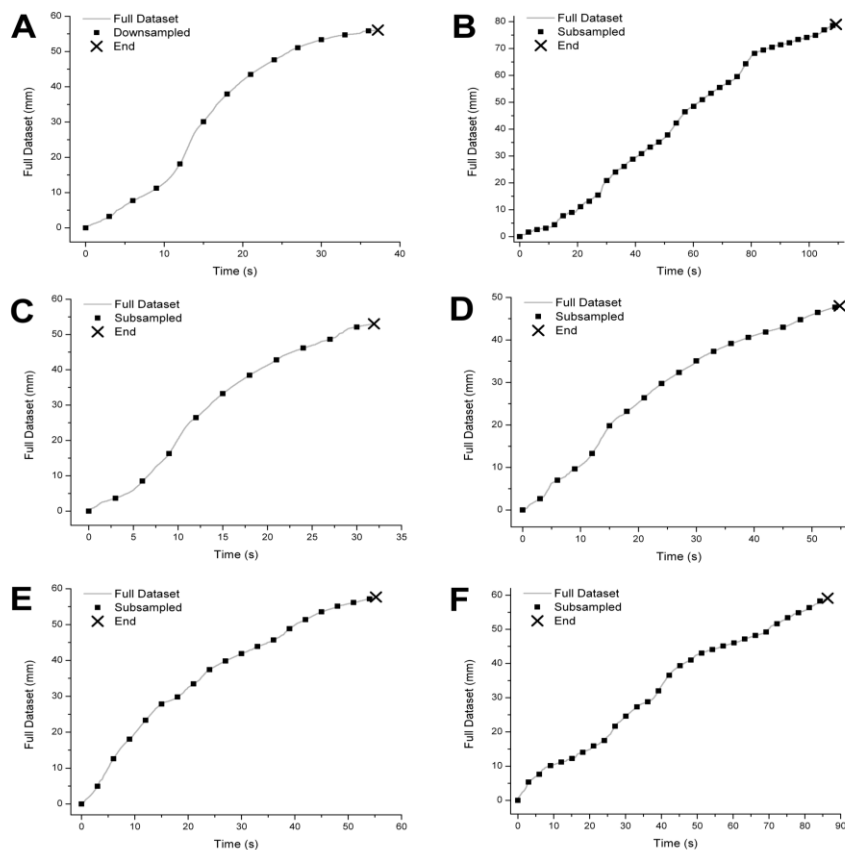


Figure S6. Tracking of all 6 droplets in Video S4 introduced in the sequence presented in table S2. (A) Droplet a, (B) Droplet b, (C) Droplet c, (D) Droplet d, (E) Droplet e, (F) Droplet f, (X) Cl^- source and end location of each droplet movement.

6. Videos Illustrating Droplet Chemotaxis

Video S1 shows the chemotactic behavior of a single ($\approx 10 \mu\text{l}$) $[\text{P}_{6,6,6,14}]\text{Cl}$ droplet. The chemoattractant in this video is a 10^{-2} M solution of hydrochloric acid (HCl). The Cl^- gradient was formed by initially filling the channel array with a 10^{-2} M solution of NaOH. At the desired destination $100 - 200 \mu\text{l}$ of the 10^{-2} M HCl was placed. After 20 s, the droplet was placed at the starting position and spontaneous movement towards the source can be observed. For convenience, the speed of the video was increased by a factor of 2.

Video S2 shows the chemotactic behavior of a ($\approx 10 \mu\text{l}$) $[\text{P}_{6,6,6,14}]\text{Cl}$ droplet. The chemoattractant in this video is an acrylamide gel which has been soaked in a 10^{-2} M solution of HCl. The Cl^- gradient was formed by initially filling the channel array with a 10^{-2} M solution of NaOH. At the desired destination the gel was placed. After 30 s, the droplet was placed at the starting position and spontaneous movement towards the gel was observed. For convenience, the speed of the video was increased by a factor of 4.

Video S3 shows the chemotactic behavior of a ($\approx 10 \mu\text{l}$) $[\text{P}_{6,6,6,14}]\text{Cl}$ droplet. The chemoattractant in this video is crystals of sodium chloride (NaCl). The Cl^- gradient was formed by initially filling the channel array with a 10^{-5} M solution of NaCl. At the desired

destination crystals of NaCl (≈ 10 mg) were placed. After 15 s, the droplet was placed at the starting position and spontaneous movement towards the dissolved crystals can be observed. For convenience, the speed of the video was increased by a factor of 4.

Video S4 shows the chemotactic behavior of 6 (≈ 10 μ l) $[P_{6,6,6,14}]Cl$ droplets. The Cl^- gradient generation is the same as in Video S1. After 15 s, three droplets are placed in different starting positions. After droplets arrive at the destination, three new droplets are placed. Upon reaching the destination, the droplets all merge to form a single larger droplet.

References

1. K. J. Fraser and D. R. MacFarlane, *Australian journal of chemistry*, 2009, **62**, 309-321.
2. S. Wellens, T. Vander Hoogerstraete, C. Moller, B. Thijs, J. Luyten and K. Binnemans, *Hydrometallurgy*, 2014, **144**, 27-33.
3. A. R. Smith, *Proceedings of the 5th annual conference on Computer graphics and interactive techniques*, 1978, 12-19.